Analyst

PAPER

View Article Online
View Journal | View Issue

Cite this: *Analyst*, 2025, **150**, 5338

Cup of Carbon: smartphone-based analysis of dissolved organic carbon in water for use in citizen science

Michael R. Muir, *[a] Adrian M. Bass,[b] Kenny Galt,[c] Kerry Morrison,[d] Lewis Robertson[d] and Emily Taylor[d]

Dissolved organic carbon (DOC) is an important component of the global carbon cycle which influences water properties such as colour and acidity. Standard methods for quantification of DOC use instruments such as Total Organic Carbon (TOC) analysers, UV/Vis spectrometers, or portable colorimeters. However, the need for specialist equipment may be a barrier to the accessibility of DOC measurement in resource limited settings. The "Cup of Carbon" method is presented as a low-cost and accessible method for the estimation of the DOC concentration of water by digital image colorimetry, using only a mug with a white interior, a laminated piece of white paper, and a smartphone digital camera. The blue pixel intensity of RGB data from digital images of water samples in mugs was used to estimate DOC concentration of water samples, and a novel white-subtraction image processing step improved the accuracy of the measurement, although also causing a decrease in measurement precision. A free R Shiny computer app was created for the fast estimation of DOC concentration from Cup of Carbon images. The Cup of Carbon method enabled good estimates of the DOC concentration of water samples from around the Silver Flowe peatland in Galloway, Southwest Scotland, from images taken by multiple users with different smartphones. Estimated DOC concentrations were within 8.2 ± 26.2% (–0.24 ± 2.07 mg L^{-1}) of the DOC concentration measured by UV/Vis spectroscopy. The simplicity and low-cost of the Cup of Carbon method make it ideally suited for the estimation of water DOC concentration in citizen science, outreach, or education settings.

Received 14th July 2025,
Accepted 28th October 2025

DOI: 10.1039/d5an00738k

rsc.li/analyst

1 Introduction

Dissolved Organic Carbon (DOC) plays a vital role in the cycling of carbon on local and global scales.[1] The term "DOC" describes the carbon atoms which form part of Dissolved Organic Matter (DOM), a complex mixture of the soluble organic degradation products of biological matter. DOM is formed of organic molecules with highly variable composition, size and functional groups which play a vital role in many chemical, biological and physical processes in fresh waters.[2] DOC facilitates the transport of carbon from terrestrial to aquatic environments,[3] is a substrate for microbial respiration in waters,[4] and influences water pH.[5] Peatland habitats, which are well known for their ability to sequester carbon for long time periods,[6] are particularly vulnerable to increased loss of carbon as DOC due to human activities such as forestry, agriculture, and wind farm construction,[7–11] as well as processes driven by anthropogenic climate change.[12] Local water quality can be significantly impacted by increased addition of DOC from peatlands, as inputs of DOC decrease pH and limit light penetration to lower depths. These impacts can in turn affect the suitability of watercourses as a habitat for species of plants, invertebrates and vertebrates.[13–16] In addition, DOC in water creates a major challenge for water companies in the UK and globally because of the dark colour given to the water by high DOC concentrations, which, despite not being harmful, is unpopular with consumers. As ~70% of water in the UK comes from upland areas where organic-rich peaty soils dominate,[17] the removal of colour forming DOC components from drinking water poses a major challenge to water companies.[12,18,19] Monitoring the DOC concentration of water is therefore vital in many settings, such as understanding the impact of human actions on the loss of carbon from peatlands

[a]*School of Social and Environmental Sustainability, University of Glasgow, Crichton University Campus, Dumfries, DG1 4ZL, UK. E-mail: Michael.Muir@Glasgow.ac.uk; Tel: +44 (0)1387 702042*
[b]*School of Geographical and Earth Sciences, University of Glasgow, Glasgow, G12 8QQ, UK*
[c]*Galloway Fisheries Trust, Fisheries House, Station Industrial Estate, Newton Stewart, Wigtown-shire, DG8 6ND, UK*
[d]*Crichton Carbon Centre, Hillhead Mill, Kirkgunzeon, Dumfries, DG2 8LA, UK*

in the form of DOC, investigating the impact of weather conditions on DOC concentration, and monitoring the quality of drinking water from peat-rich areas.

The standard method of quantifying DOC in water involves direct analysis of carbon using a Total Organic Carbon (TOC) analyser. These instruments oxidise the organic components of DOC, usually with chemical (*e.g.* with persulphate) or high temperature oxidation methods, and then measure the concentration of gaseous CO_2 generated by IR absorption.[20] Alternatively, the light absorbing properties of water at UV or visible wavelengths can be analysed as a proxy for DOC, as the absorbance properties of water have been demonstrated to be directly correlated to DOC concentration.[21,22] While the absorbance methods are generally cheaper and more accessible than the direct DOC analysis methods, both techniques require access to specialist instrumentation and laboratory analysis. Field measurements of DOC can be made using portable spectrophotometers or colorimeters, which are lower cost forms of these instruments.

The widespread availability of high-quality digital cameras in smartphones has created an opportunity to create low-cost and broadly accessible analytical methods which use the digital camera of a smartphone to replace costly or specialist sensors in colorimetric analysis. These techniques, sometimes referred to as digital image colorimetry[23,24] are Digital Image Analysis (DIA) methods suitable for enhancing analytical capability in resource-limited settings[25,26] and have been applied to the analysis of nutrients in water and soils,[27,28] soil salinity,[23] potentially toxic elements (PTEs) such as Hg in water,[29] as well as in medical,[30] and citizen science settings.[31] Citizen science has been identified as a valuable tool in environmental science and water quality research which can enable projects to have a wide geographical distribution, increase levels of engagement with members of the public and policymakers, and generate large datasets.[32,33] Low-cost citizen science methods also provide an opportunity to collect data with good temporal and spatial resolution which is useful in peatlands where there can be variable water quality over short distances and timescales.[10] The benefits of citizen science, and the potential for smartphone-based analysis for quantification of DOC in water, has been recognised previously. Examples of the use of smartphones as analytical instruments in DOC analysis include their use to measure colour and reflectance of surface and coastal waters *in situ*.[34–38] However, these methods have limitations, such as only being able to analyse deep water due to image interference from the underlying bed of shallow waters,[34,35] or requiring specialist hardware or adaptations to the smartphone.[36–38] The currently reported methods are either not applicable to peatland areas, as the depth of upland streams around peatlands are often too shallow for the methods to succeed, or have limited applicability for citizen science applications due to the hardware adaptations required. To address these limitations, a novel method: "**Cup of Carbon**" is presented in which an ordinary ceramic mug with a white interior is used for photographing water samples to help standardize digital images, remove the water depth requirement and enable the method to have broad applicability for citizen science applications. The method has been applied to the analysis of organic-rich waters in an area of blanket peat in Southwest Scotland and has the potential to be used for citizen science applications to monitor DOC in surface water and tap water. The aims of this project were: (1) to develop the novel Cup of Carbon method and demonstrate its effectiveness for quantifying DOC in water samples, and (2) to implement the Cup of Carbon method to estimate DOC in freshwater from a water catchment with peaty soils using data collected by citizen scientists.

2 Materials and methods

2.1 Method development and proof of concept

The relationship between DOC concentration and digital image red, green and blue (RGB) pixel intensity was first investigated by preparation of a set of 33 solutions of increasing DOC concentration. A solution with a significant dark brown colour was prepared by extracting DOC from soil using deionised water in a 1 : 20 (w/v) ratio. Three replicates of ~10 g of field-wet garden soil were weighed into conical flasks and 200 ml of deionised water added. The flasks were stirred with a magnetic stirrer for 2 hours, after which the solutions were allowed to settle for 30 minutes and were subsequently filtered under vacuum using Buchner apparatus and filter papers (no. 1, Whatman). The strongly coloured soil DOC extracts were combined and used as a concentrated stock solution for further analysis. To create solutions of increasing DOC concentration, a ceramic mug with a volume of ~300 ml, depth of ~8.5 cm and a white interior, was filled to near the brim with colourless deionised water (volume ~300 ml, depth ~8.5 cm). Repeated additions of 10 ml of the highly coloured DOC stock solution were made, incrementally increasing the colour and DOC concentration of the water in the cup. Photographs were taken with a mid-range smartphone (Samsung Galaxy A20E) after each addition. Samples were also collected from the mug after each addition for analysis by UV/Vis spectroscopy, and a further addition of 10 ml of DOC stock solution was made, incrementally increasing the DOC concentration of the test water sample. A set of 11 additions were made and the procedure was repeated 3 times, leading to 33 digital image and UV/Vis data points with varying DOC concentration. Pictures were taken outdoors in daylight but not in direct sunlight, to try and ensure reproducible lighting conditions between the samples.

2.2 Cup of Carbon measurement procedure

Following the proof of concept testing, the Cup of Carbon measurement procedure was developed for use in the field by citizen scientists. The procedure for collection of Cup of Carbon data was designed to be as simple as possible, requiring only a straight sided, cylindrical ceramic mug with a white interior, volume of ~300 ml, and internal height of 8–9 cm (mean internal height of 13 randomly selected mugs fitting

the method description = 8.7 ± 0.25 cm). The mugs were rinsed several times with sample water, then filled as close to the brim as possible with water sample (~8.5 cm depth) and placed on a laminated white piece of white paper to be the image background. No filtration step was used before analysis as DOC is known to be the dominant component influencing the brown colour of waters in upland catchments with peaty soil type,[39,40] and the water samples were seen to be transparent with low turbidity (see SI 3). Digital photographs of the mug were then collected from a height of around 40–80 cm above the mug using a smartphone digital camera. The height of the camera above the mug was not fixed, but was far enough away to allow the full piece of paper under the mug to be framed within the image. The images were taken in daylight but not in full sunlight, with the whole image area in shade (under cloud or shaded by a large object) to minimise reflections and glare from the sun on the water surface and on the laminated white paper background. An example of the image collection procedure and cup image are shown in Fig. 1.

2.3 Analysis of field samples using the "Cup of Carbon" method

Samples were collected from around the Silver Flowe peatland in Galloway, SW Scotland. Two visits were made to the site, in March and August 2023, as part of an ongoing water monitoring project, "Peatland Connections".[41] The Cup of Carbon analysis was conducted as part of a science outreach activity with members of the public and peatland and fisheries professionals from the Crichton Carbon Centre and Galloway Fisheries Trust. The Silver Flowe, which covers an area of ~620 hectares, is one of the least disturbed areas of deep peat in Southwest Scotland and is registered as a Site of Special Scientific Interest (SSSI).[42] However, areas nearby the protected site have been impacted by historic activities such as drainage, peat cutting and forestry and, during the site visits in 2023, there was evidence of disturbance to the peat soils nearby from forestry clear-felling activity. Water samples were collected from 16 small streams and drainage ditches flowing into and out of the peatland area (Fig. 2). A total of eight participants took part in the Cup of Carbon analysis, including the lead researcher, 4 industry professionals and 3 citizen scientists (5 people were present on each trip, 2 of whom took part in both trips.). Digital photographs of the sample-filled mugs were taken by each participant using their own smartphone using default image acquisition settings. Four different mugs were used during the data collection. A total of 118 Cup of Carbon images were taken by 5 smartphones from 16 sample points in March and 5 smartphones from 11 sample points in August (not all participants took a picture of every sample, while multiple replicates were measured at some sample points). After returning from the field, the digital images were collected and analysed (section 2.3). Additional water samples from each sampling point were also collected in 50 ml centrifuge tubes and returned to the lab for further analysis.

2.4 Digital image analysis

To analyse the image data, an R[43] shiny app: "Cup of Carbon – estimation of Dissolved Organic Carbon (DOC) from images", was developed using RStudio[44] using the shiny,[45] shinyfiles,[46] and imager[47] R packages. The desktop app enables a user to select a folder containing Cup of Carbon images, click the "water" (centre of cup) and "paper" (white paper background) regions of the image, and then extracts the average RGB values for the selected region based on a square with a defined pixel

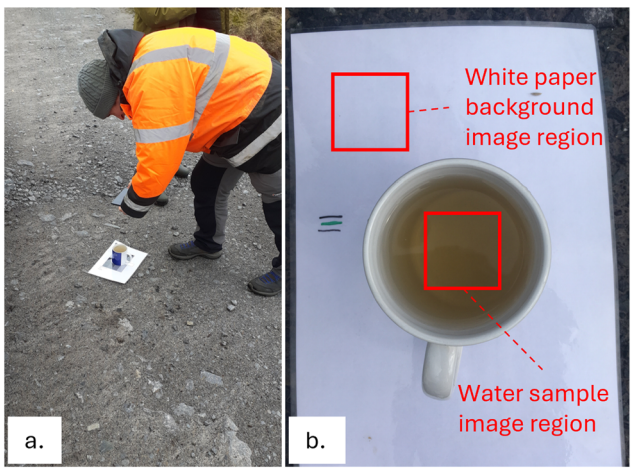

Fig. 1 a. Example showing how the images of cups containing water samples were collected in the field. b. Example image of cup containing water sample showing the water sample and white paper background image regions.

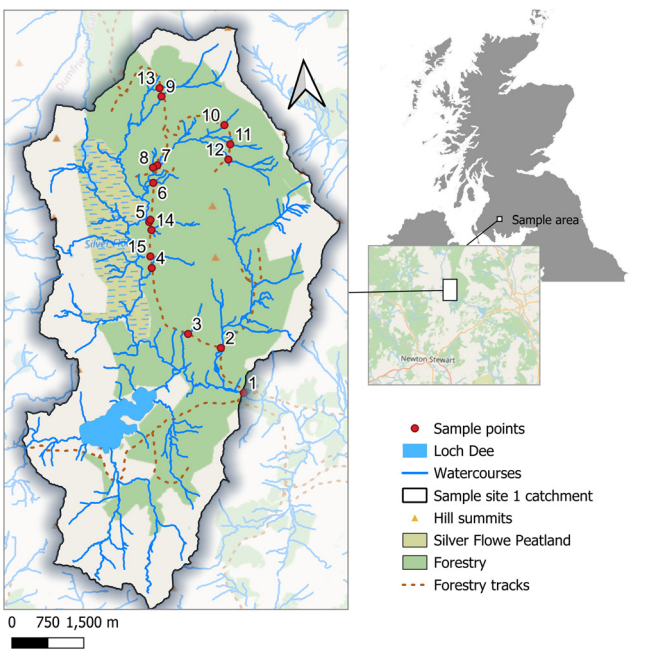

Figure contains spatial data from Openstreetmap (2025) and Ordnance Survey (2025)

Fig. 2 Map showing the location of sample points.

area (*e.g.* 200 by 200 pixels) (Fig. 1b). The relatively large image sampling area means that variations in image colour, such as the shadow in the water sample region of Fig. 1b, are averaged so that small inconsistencies in image quality don't negatively impact the analysis. The RGB values for the "water" and "paper" regions are stored in a table which can be exported, along with the estimated DOC concentration, which is calculated based on the calibration method discussed below, using the "white subtracted" (B_{ws}) image processing method (section 2.4.1). A screenshot of the app is shown in SI Fig. S1, and the app, code and example images are available with the SI.

2.4.1 Image processing. In addition to using raw, unprocessed image RGB data, two image processing methods were tested in an attempt to reduce artefacts in the data from variable lighting conditions or differences between smartphone camera sensors. Both of the image processing methods tested required gathering the RGB intensity from a section of image which contained the water sample in the cup, and a second image section which contained the white laminated paper background (Fig. 1b). A perfectly white section of the image theoretically would have RGB = [255, 255, 255], however in practice the white paper areas of the sample images were always slightly off-white, due to variations in image quality, and the RGB values of the white paper background varied from ~175–245. This was mainly due to variations in the brightness of the collected images due to variable daylight conditions and varying sensitivity of the cameras of different smartphones. The first image processing method tested was a white balancing (WB) method in which the expected RGB values for a fully white section of image (RGB = [255, 255, 255]) are divided by the measured RGB values of the white paper background to generate a correction factor which is then multiplied by the RGB value of the sample section of the same image.[48,49] A second novel image processing procedure was also developed, based on the assumption that any variation in the RGB colour of the white background would be consistent across the whole image. To correct the images, the measured white paper R, G and B values were subtracted from 255 to generate a correction factor for the R, G and B data for each image. The correction factor was then added to the R, G and B data from the analysis of the water sample in the cup. For example, if the white paper background of an image collected had RGB = [196, 207, 231], a correction factor would be generated from these values by subtracting each from 255, to give correction factors of 59, 48 and 24, for R, G and B, respectively. If the sample data measured for the same image had RGB = [117, 100, 72], then the appropriate correction factor would be added to each number, to give a corrected RGB value = [176, 148, 96]. This processing method, referred to as the white subtraction (WS) method, corrects the collected sample data for variations to do with the brightness or darkness of the image due to variable lighting conditions or the performance of different camera sensors. Therefore, a total of three DIA methods were applied to each calibration and sample image: Uncorrected (U), White Balanced (WB), and White Subtracted (WS). The accuracy and precision of results using each of the three DIA methods was investigated to identify which performed best for the estimation of DOC in water samples.

2.4.2 Calibration. A series of calibration standards was prepared by serial dilution of a high DOC concentration water sample collected in the field in August 2023. 1000 ml of highly coloured water sample from Silver Flowe peatland was collected in a plastic bottle, filtered through glass fibre filters (VWR) using Buchner filtration apparatus, and refrigerated for further analysis. This solution (DOC concentration measured by TOC analyser = 65.54 mg L^{-1}, standard deviation of 3 replicates = 0.78 mg L^{-1}) was diluted to create a series of 12 standard solutions which were analysed by UV/Vis and the Cup of Carbon method, with 5 replicate images collected for each of the 12 standards. The calibration graphs created were used to estimate the DOC concentration of unknown samples by the Cup of Carbon method.

2.5 Analysis of DOC

The DOC concentration of all samples was analysed by UV/Vis spectroscopy using a VWR UV-6300PC spectrophotometer with a matching pair of quartz cuvettes (10 mm path length) and deionised water in the reference cuvette. Cuvettes were rinsed with deionised water and several volumes of sample before the spectra were collected. Scanned absorbance spectra were collected from 800–200 nm in 0.5 nm intervals. DOC concentration was calculated from the UV/Vis absorbance spectra using the two-component model of Carter *et al.*, (2012)[22] which estimates the DOC from the absorbance at 2 wavelengths (270 and 350 nm) based on a model paramaterised with ~1700 surface water samples from the UK and North America. In addition, 11 water samples collected in August were also measured using a TOC analyser (Thermolox, Sercon) and compared with the UV/Vis method for quality assurance. The DOC quantification for these 11 samples by the UV/Vis method compared favourably with the TOC analyser results, with an average recovery of 104.30% and results within the 95% confidence intervals reported by Carter *et al.*, (2012)[22] (see SI 2).

2.6 Data analysis

2.6.1 Analysis of blank and replicate samples. The method limit of detection was evaluated by analysis of 10 blank (0 mg L^{-1} DOC) solutions using the Cup of Carbon method, with comparison between each of the 3 image processing options (U, WS and WB). The LOD was calculated from the mean of the blank measurements + 3 standard deviations. Similarly, 10 replicates of 2 sample solutions (a low DOC solution of 4.27 mg L^{-1} and medium concentration DOC solution of 8.63 mg L^{-1}) were measured to investigate the accuracy and precision of the Cup of Carbon method with each image processing option. The standard deviation and relative standard deviation (standard deviation as a percentage of the sample mean, RSD) of the replicates were calculated to indicate method precision, and the accuracy was investigated by calculating the percentage recovery of each sample by dividing the mean of the DOC concentration from the Cup of Carbon

method by the DOC concentration measured by UV/Vis and multiplying by 100. To determine whether the Cup of Carbon method could successfully distinguish between the water samples with moderate differences in DOC concentration, a one-way ANOVA with Tukey's HSD *post hoc* test was applied to the blank, low and medium DOC concentration solutions.

2.6.2 Analysis of field samples. Data analysis and visualisation was carried out using MS Excel,[50] Minitab[51] and RStudio.[43,44] Scatter graphs and regression analysis were used to investigate the relationship between the Cup of Carbon method and DOC measured by UV/Vis. The Bland–Altman (B–A) limits of agreement (LoA) method[52] was used to test the agreement of the novel Cup of Carbon with the reference UV/Vis method using the Minitab Bland–Altman plot macro. The B–A plot shows the mean of the measurement of a sample by both the novel and standard methods (x axis) plotted against the measurement by the novel method subtracted from the standard method (y axis). An offset of the mean difference from zero on the y axis indicates a systematic bias in the results of the novel method compared to the reference method. Limits of agreement on the B–A plot show the upper and lower range that is likely to contain 95% of the data calculated by the novel method. The LoA indicate the precision of the novel method compared to the standard method, with narrower LoA around the mean difference line indicating better precision of the novel method and wider LoA indicating poorer precision. As a further assessment of the overall accuracy and precision of the Cup of Carbon method, the Concordance Correlation Coefficient (CCC) was calculated[53,54] using the DescTools R package.[55] The CCC is a reproducibility index which summarises the accuracy and precision of a novel method with a single value, r_c, by comparing the deviation of plotted data from the 1 : 1 line. The r_c can have a value of $r_c = -1 \geq 1$, with a value closer to 1 indicating a positive relationship with good precision and accuracy, values close to −1 indicating a negative relationship with good precision and accuracy and values closer to zero indicating a weak or no relationship. A scatter plot with all values falling exactly on the 1 : 1 line would have $r_c = 1$. Information about the accuracy of the data is captured by the bias correction factor (C_b) which can take values between 0 and 1, with values closer to 1 indicating greater accuracy and values closer to 0 indicating poor accuracy. The C_b can be further broken down into two terms, the location shift ($\hat{u}$), which is a value that describes any systematic deviation of the measured points above or below the 1 : 1 line, and the scale shift ($\hat{v}$), which describes any deviation in the angle of the modelled regression compared to the 45° angle of the 1 : 1 line on a square plot. Smaller values of $\hat{u}$ indicate less location shift, and therefore greater accuracy, while larger positive or negative values indicate a greater deviation from the 1 : 1 line. Values of $\hat{v}$ closer to 1 indicate less scale shift, while values greater or less than 1 indicate a greater deviation from the 45° angle of the 1 : 1 line. Precision is captured by the Pearson correlation coefficient. More information about the derivation and interpretation of these parameters is given in ref. 53 and 56.

2.7 Investigating variation between users

To investigate the variation in results between different users, each with a different smartphone, linear mixed models (LMM) were created using the "lme4" package in R.[57] Three models were run with the results of each of the DIA options (B, B_{WB}, or B_{ws}) used as the response variable. "phone" was included as a fixed effect to investigate the differences between users each with a different phone, and "sample site" (*e.g.* the numbered sample locations, 1–16) was included as a random effect. Significant differences between the "phone" variable were identified using the "lmerTest" package in R.[58]

3 Results

3.1 Proof of concept

The increasingly dark brown colour of samples with increasing DOC concentration was evident in the digital images taken of mugs filled with samples prepared from the soil extract solution (Fig. 3). This variation in colour was reflected in the RGB values of the "water sample" region of the images within the mugs for 33 samples prepared from the soil extract DOC solution (Fig. 4). The R, G and B values all decreased as the colour changed from light to dark, with the B channel showing the largest decrease. A qualitative interpretation shows that there is an inverse relationship between DOC concentration and B pixel intensity.

The intensity of the B channel measured by DIA showed a negative exponential relationship with DOC ($R^2 = 0.98$, residual standard deviation (sd) = 3.51). The G data also fitted a negative exponential relationship with DOC, although the fit was slightly weaker than for B ($R^2 = 0.90$, residual sd = 5.18), and the data covered a narrower range. The intensity of the R

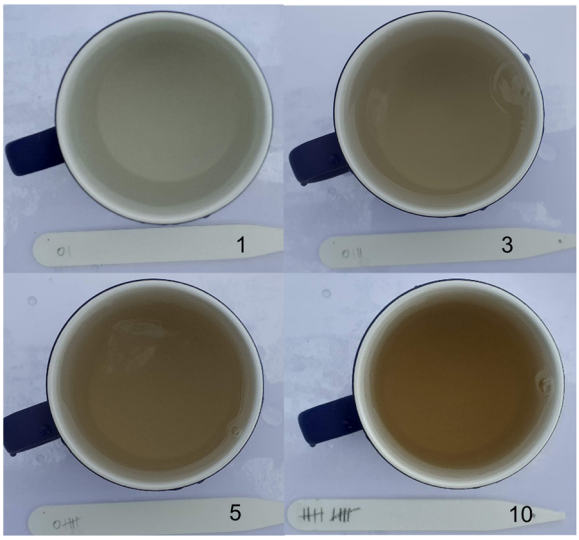

Fig. 3 Example images of 4 of the 33 samples used for method development. The numbers 1, 3, 5 and 10 relate to the number of 10 ml additions of soil extracted DOC solution added.

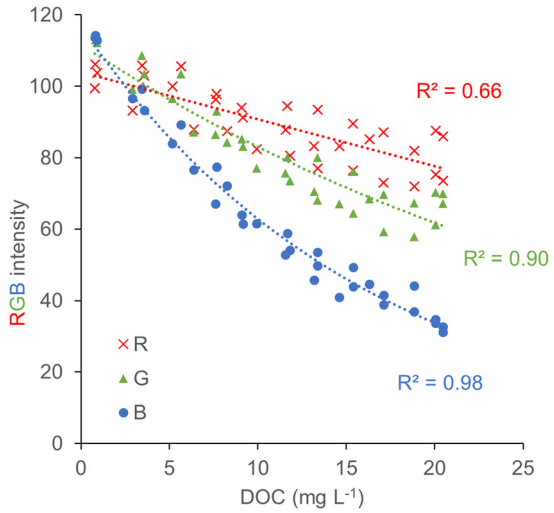

Fig. 4 Scatter plot of digital image analysis R, G and B data from images of increasing concentrations of extracted soil solutions. Regression lines show the B and G data fitted with exponential models, while the R data is fitted with a linear model.

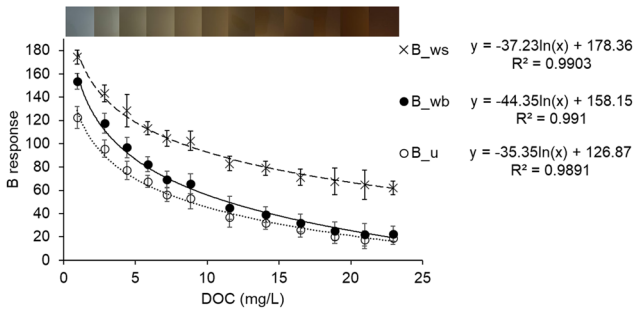

Fig. 5 Calibration graphs showing the relationship between Cup of Carbon measurements and DOC. Calibration curves were generated using logarithmic regression fitted to data from uncorrected (B_u), white balanced (B_wb) and white subtracted (B_ws) pixel data from images of peatland DOC solutions with known concentration. The colour bar at the top of the graph shows an example of the water sample region analysed for each point on the graph.

channel also decreased with increasing DOC concentration, although less than the B and G channels. The R channel showed a negative linear correlation with DOC, although the lower R^2 value of 0.66 and higher residual sd of 5.88 highlights the greater spread of the data compared to B or G.

The analysis of the DOC extracts indicated that the Cup of Carbon method could be useful for estimation DOC in unknown samples using the B pixel colour channel, and therefore this was focused on for further data analysis. The U, WB and WS DIA methods (section 2.4.1) were applied to the B pixel data, and are referred to as B_U, B_{WB}, and B_{ws}, respectively.

3.2 Method calibration and image processing

The B_U, B_{WB} and B_{ws} DIA data for 5 replicate images of 12 calibration standards was plotted against the DOC concentration in order to create calibration graphs (Fig. 5), with data found to fit negative logarithmic models.[59] The B_{WB} data had the highest R^2 value out of the 3 image processing methods tested (R^2 = 0.991, residual sd = 3.98). The B_{ws} image data had the next highest R^2 value (R^2 = 0.990, residual sd = 3.48), followed by the B_U data, which had a slightly lower value (R^2 = 0.989, residual sd = 3.51). The calibration plots for all three image processing methods showed acceptable qualities to be used for the estimation of unknown samples, with high R^2 values, and evenly distributed residuals. Therefore the calibration models, which were generated using a single smartphone (Samsung Galaxy A20e), were then applied to calibrate Cup of Carbon water sample data collected using different smartphones.

3.2.1 Limit of detection, precision, and accuracy. Analysis of replicate samples of blank (0 mg L^{-1}), medium (8.63 mg L^{-1}) and low (4.27 mg L^{-1}) concentration DOC solutions identified differences between the DIA options used for analysis (Table 1, and SI Fig. S5). The boxplots from the replicate analysis of test samples (Fig. S5) show that there were clear differences evident between the blank, medium and low concentration samples in all the DIA options tested as all the measurements are clustered close to the true values. However there was variability in the accuracy and precision of results using the different DIA options. B_U had slightly higher LOD than B_{WB} and B_{ws}, respectively. Using B_U also over-estimated the concentration of the medium DOC sample, although the precision of the replicate measurements was the relatively good, and the accuracy of the analysis of the low DOC sample was also good. The B_{WB} DIA option was similar to the results of B_U, with excellent estimation of the low DOC sample concentration and over-estimation of the medium DOC sample. The estimation of DOC using B_{ws} had a low LOD, excellent

Table 1 Limit of detection (LOD), precision (RSD%) and accuracy of replicate (n = 10) measurements of blank (0 mg L^{-1}), medium (8.63 mg L^{-1}) and low (4.27 mg L^{-1}) concentration DOC samples using the three digital image analysis options tested

	Blank (0 mg L^{-1})				Medium DOC (8.63 mg L^{-1})				Low DOC (4.27 mg L^{-1})			
Method	Mean	SD	RSD (%)	LOD	Mean	SD	RSD (%)	Recovery (%)	Mean	SD	RSD (%)	Recovery (%)
B_U	1.53	0.30	19.61	2.42	11.04	1.45	13.10	128.02	4.59	0.79	17.20	107.51
B_{WB}	1.38	0.26	18.84	2.16	11.23	1.62	14.39	130.12	4.34	0.73	16.89	101.74
B_{ws}	1.21	0.22	18.18	1.86	8.75	2.67	30.50	101.41	3.38	0.85	25.05	79.21

B_U = uncorrected B pixel data, B_{WB} = white balanced B pixel data, and B_{ws} = white subtracted B pixel data.

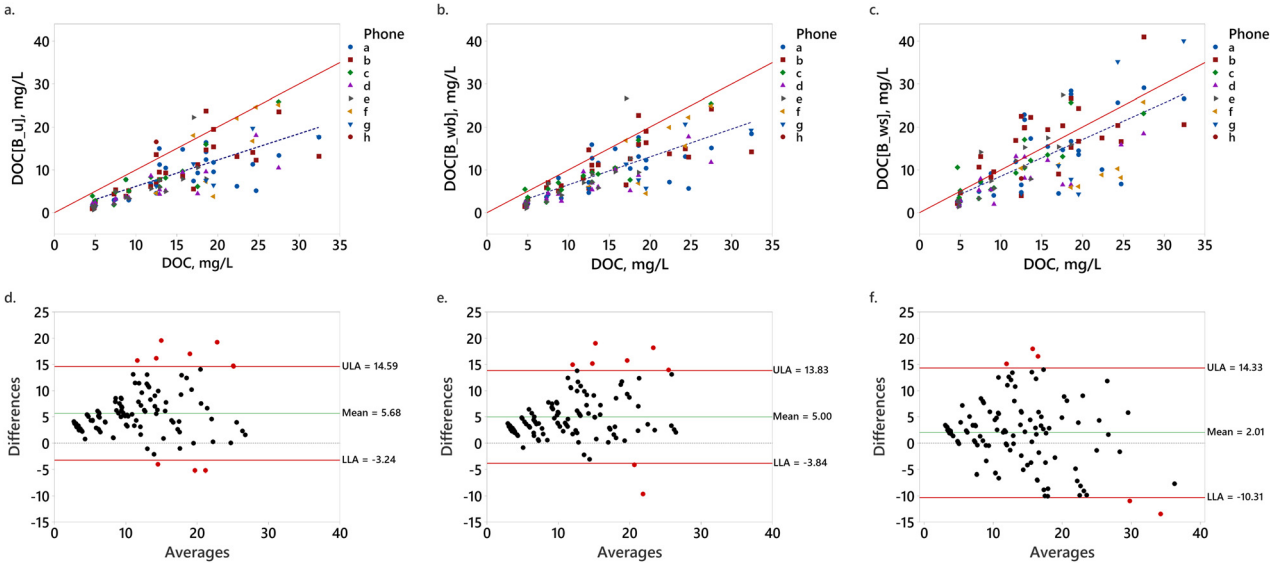

Fig. 6 Comparison of the DOC concentrations for the Silver Flowe samples estimated by the Cup of Carbon method with that measured by the UV/Vis method. (a–c) Scatter plots comparing the measured DOC concentration by UV/Vis with that estimated by the Cup of Carbon method using the uncorrected B pixel data (B_U), the B pixel data with white balance correction (B_{WB}), and the B pixel data with white subtraction correction (B_{ws}), respectively. Red line on each plot shows 1 : 1 line, and blue dashed line on each plot shows the regression fit for the Cup of Carbon data. (d–f) Bland–Altman limits of agreement plots comparing the measured DOC concentration by UV/Vis with that estimated by the Cup of Carbon method using B_U, B_{WB}, and B_{ws} digital image data, respectively. Red lines on each plot show the Bland–Altman limits of agreement and the green line shows the mean difference between the Cup of Carbon and UV/Vis methods.

accuracy for the medium DOC sample, and acceptable accuracy for the low DOC sample. However, the precision of the B_{ws} DIA option was poorer than the other two DIA methods tested, with the highest standard deviation and RSD values for the DOC samples. Despite the high RSD values indicating relatively poor precision, ANOVA tests with Tukey's HSD *post hoc* testing identified that all 3 of the DIA options applied could identify significant differences in DOC concentration between the blank, low and medium DOC samples ($p < 0.05$) (SI 4). The analysis of the blank and replicate sample solutions showed that the Cup of Carbon method showed promise for the accurate quantification of DOC in water samples, with no clear evidence of one DIA option outperforming the others, therefore the Cup of Carbon method was used to quantify samples from around the Silver Flowe peatland with all three DIA options applied for comparison.

3.3 Analysis of water samples from around Silver Flowe peatland

From the two visits to the sample site, there were 118 individual digital image data points collected by 8 different smartphones to compare with 24 DOC measurements. The data from the different smartphones was calibrated using the appropriate equation from the graphs in Fig. 5. The results of analysis of the samples by the Cup of Carbon method and UV/Vis are presented in Fig. 6. The three DIA methods (B_U, B_{WB}, and B_{ws}) led to varying accuracy and precision in the prediction DOC. The Cup of Carbon results were strongly correlated with DOC for all three DIA methods tested, with correlation coefficients of >0.69 in all cases ($p < 0.001$) (Table 2). However, there were differences in the accuracy of the DIA methods applied. Using B_U to predict DOC showed a systematic negative bias, demonstrated by the values falling below the 1 : 1 line in Fig. 6a. Using B_{WB} also showed a similar, but less pronounced negative bias (Fig. 6b). The estimation of DOC using B_{ws} showed the best accuracy, with points more evenly distributed around the 1 : 1 line, but still with a slight underestimation of sample DOC concentrations and a broader spread of data indicating lower precision, particularly at concentrations below 20 mg L^{-1}, compared to B_U and B_{WB}. This interpretation is supported by the B–A plots (Fig. 6d–f), which show the DOC estimates using the B_U and B_{WB} image data having a mean difference of 5.68 and 5.00 mg L^{-1}, respectively, while using the B_{ws} image data led to a lower mean difference of 2.01 mg L^{-1} compared to the DOC measured by UV/Vis, highlighting the greater accuracy of the B_{ws} DIA method. The B–A plots

Table 2 Results of CCC analysis for the DIA options using uncorrected (B_U), white subtracted (B_{ws}), and white balanced (B_{WB}) B pixel data

Method	r_c (±95% CI)	C_b	$\hat{\nu}$	$\hat{u}$	r
B_U	0.567 (0.471, 0.651)	0.729	0.871	−0.852	0.779
B_{ws}	0.664 (0.557, 0.750)	0.953	1.201	−0.257	0.698
B_{WB}	0.602 (0.505, 0.684)	0.771	0.856	−0.756	0.781

r_c = Concordance Correlation Coefficient (CCC). 95% CI = lower and upper 95% confidence intervals for r_c. C_b = Bias correction factor. $\hat{\nu}$ = scale shift. $\hat{u}$ = location shift relative to the scale. r = Precision coefficient (Pearson's r).

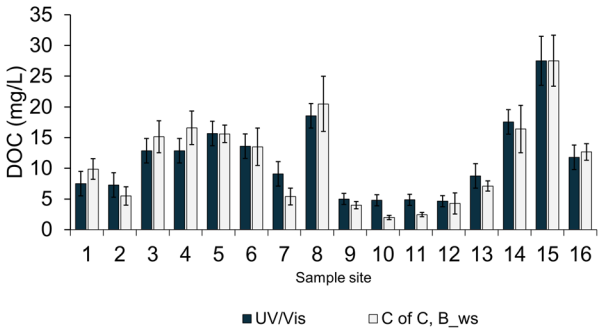

Fig. 7 Bar graph showing the comparison of DOC measured by the UV/Vis and Cup of Carbon methods at all 16 sample sites in March. Bars of Cup of Carbon results show the mean of all measurements made using all phones in March (using the white subtraction image processing method, B_{ws}) with error bars showing calculated 95% confidence intervals. The error bars on the estimate of DOC concentration using the UV/Vis method show the 95% confidence intervals reported by Carter *et al.*, (2012)[22] of 0.9, 2 and 4 mg L^{-1} for ranges of DOC concentration from 0–5, 5–20 and 20–80 mg L^{-1}, respectively.

identify B_{WB} as having the lowest spread of data, with a 95% confidence interval around the mean of 8.83, compared to 8.91 and 12.32 for the estimates using the B_U and B_{ws} image data, respectively. To support the graphical interpretation of the comparison between the Cup of Carbon and the reference UV/Vis methods, the Concordance Correlation Coefficient (CCC)[53,54] was calculated to determine which DIA method showed the best precision and accuracy (Table 2).

The results of CCC analysis corroborate the interpretation of the scatter and B–A plots, showing that using B_U to estimate DOC has the lowest accuracy, with a bias correction factor of $C_b = 0.729$, while B_{ws} had the best accuracy, with a $C_b = 0.953$. The improved accuracy of B_{ws} is related to the relatively low scale shift value of $\hat{\nu} = -0.257$, while the larger magnitude of the location shift values for B_U and B_{WB}, of $\hat{u} = -0.852$ and -0.756 respectively, show the greater deviation of the Cup of Carbon estimates from the reference method using these DIA options. However, the precision of the DIA methods shows a different pattern, with B_{WB} having the highest correlation coefficient of $r = 0.781$, and B_{BU} and B_{ws} having lower values of 0.779 and 0.698, respectively. The accuracy and precision of the three DIA options are captured by the concordance correlation coefficient (r_c), which shows that the overall method precision and accuracy decreases in the order $B_{ws} > B_{WB} > B_U$. This highlights that both the B_{ws} and B_{WB} DIA options improved the estimate of DOC by the Cup of Carbon method compared to using the uncorrected B_U image data. The results of the comparison of DIA methods also demonstrate that finding an appropriate DIA process which optimizes both accuracy and precision is challenging, as the improvement of accuracy of the B_{ws} image processing method came at the expense of decreased precision. Method precision may be improved by additional replicate measurements, and a key benefit the Cup of Carbon method, and other smartphone-based digital image colorimetry methods, is that their low cost and ease of use makes replicate measurements to improve the quality of results very achievable.[34] The graph in Fig. 7 shows the mean of the DOC estimates by the Cup of Carbon method using B_{ws} image processing for the 16 sample points measured in March compared to the DOC measured by UV/Vis (error bars show 95% confidence intervals). The results demonstrate that the accuracy of the B_{ws} DIA option allows good estimation of the DOC concentration of samples by calculating the mean of replicate measurements. The mean accuracy of the results from the Cup of Carbon method shown in Fig. 7 was 91.8 ± 26.2% (mean absolute error = −0.24 ± 2.07 mg L^{-1}), and mean RSD% of replicate measurements was 39.0 ± 15.7%.

3.4 Investigating variation between users

The summary of the linear mixed model used to investigate variation in the estimate of DOC between phones using the B_{ws} DIA option is shown in Table 3, while the outputs for the models based on B_U and B_{WB} are shown in SI Tables S3 and S4. Model residuals showed a slight positive skew (median = −0.13, min = −2.46, max = 3.03), and Levene's test for equal variances indicated moderate heteroscedasticity (df = 7, F = 2.12, $p = 0.047$) which, on examination of boxplots of residuals grouped by phone, appears to be due to high variance in phone G and low variance in phone H. LMMs are able to cope with moderate violations of normality and homoscedasticity, and comparison with a robust linear mixed model using the "robustlmm" R package led to the same interpretation, therefore the results of LMM analysis are presented. For the B_{ws} LMM, residual model variance was 30.59 ± 5.53 (variance ± standard deviation), while sample site, included in the model as a random effect, had a variance of 48.97 ± 7.00, indicating considerable between-site variation. Examining the differences between phones showed that phone D was significantly lower than phone A, while phones B and F showed moderate differences ($p < 0.1$). Phones C, E, G and H were not significantly different. This indicates that there was some variation between phones, but that only phone D showed statistically significant difference at a $p < 0.05$ level. The LMMs using B and B_{WB} esti-

Table 3 Results of LMM analysis using the white subtracted (B_{ws}) DIA option to compare the variation in estimates of DOC between phones. DOC estimated by B_{ws} was the response variable, with "phone" as a fixed factor and sample site as a random factor. The estimated intercepts of phones B–H are compared against phone A for significant difference, while the intercept of phone A is compared to 0

Phone	Intercept (±SE)	df	t value	p value	Significance
A	12.96 ± 2.06	22.98	6.29	<0.001	***
B	2.58 ± 1.52	93.49	1.70	0.093	
C	−2.44 ± 1.76	93.80	−1.39	0.169	
D	−5.34 ± 1.73	93.80	−3.09	0.0026	**
E	−2.14 ± 1.76	93.89	−1.21	0.229	
F	−4.12 ± 2.26	94.13	−1.82	0.072	
G	3.71 ± 2.54	94.05	1.46	0.148	
H	0.21 ± 5.83	94.28	0.04	0.972	

SE = standard error. df = degrees of freedom. Significance codes: *** $p < 0.001$; ** $p < 0.01$; * $p < 0.05$.

mations of DOC as the response variables (Tables S3 and S4) identified phones D, F and H, as being significantly different to phone A ($p < 0.05$). This highlights that the B_{ws} DIA option improved the results of phones F and H compared to the B or B_{WB} DIA options, however they also show that phone D consistently gave low estimations of DOC. Following LMM analysis, the reason for the significant difference in the estimations from phone D was investigated. Looking at the original photographs used during data collection revealed that the images collected with phone D were taken with the phone flash switched on (as indicated by reflections in the image on the water surface and paper background, see SI, Fig. S6) which appears to have led to a lighter coloured image of the water and lower B pixel intensity. This highlights that care must be taken to ensure that citizen science methods are as robust as possible to user variation.

4 Discussion

4.1 Digital image analysis for assessment of DOC concentration

DIA methods using smartphone digital cameras potentially offer a low-cost and accessible alternative to lab-based methods for environmental monitoring.[26] The novel "Cup of Carbon" method demonstrated a clear relationship between the RGB values of digital images and increasing DOC concentration, with the intensity of the B pixels showing the strongest relationship with DOC concentration. This is in agreement with Zeng *et al.*, (2021) who found that increasing concentration of humic acid in aqueous solution had a stronger effect on B pixels than R or G in a smartphone-based DIA method for water analysis using a custom sample enclosure.[38] The natural logarithm of uncorrected and corrected B pixel data showed strong negative logarithmic relationships with DOC concentration in standards prepared by serial dilution of a high DOC water sample (Fig. 5), with R^2 values decreasing in the order B_{WB} ($R^2 = 0.991$) > B_{ws} ($R^2 = 0.990$) > B_U ($R^2 = 0.989$). These samples were suitable for method calibration to estimate the concentration of DOC in unknown samples, although the fact that the calibration was prepared using only 1 smartphone and was then applied to images collected by different models of smartphone used by multiple users likely led to a decrease in accuracy and precision of results, as ideally an individual calibration would be created for each smartphone.[60,61] However, LMM analysis showed that only phone D had a significant difference to phone A at a $P < 0.05$ level, which indicates that the use of a single calibration graph made using phone A was acceptable for the estimation of DOC with most of the phones used. Both the B_{WB} and B_{ws} image processing methods led to varying extents of improvement of the accuracy of the DOC estimation in the sample analysis and, although the novel B_{ws} image processing method caused a decrease in the measurement precision, the concordance correlation coefficient of $r_c = 0.664$ identified B_{ws} as giving the best DOC estimate of the DIA methods tested (Table 2). Digital image analysis can be sensitive to experimental conditions such as fluctuations in lighting or camera quality[62] which can effect the precision and accuracy of results compared to standard methods.[23,63] Image processing methods using a reproducible section of sample images, such as a colour calibration card or white balancing with a white section of the image background, have previously been demonstrated to improve the accuracy of DIA methods by correcting for artefacts in lighting and image quality. Many studies have applied colour correction to images used for analysis of environmental, medical and chemical samples using greyscale or colured calibration cards.[23,26,38,49,60,64] The B_{ws} DIA method showed a good ability to improve inaccurate data due to varying image quality and lighting levels, with the simple requirement of using a white image background. The novel B_{ws} DIA method presents a promising way to correct for variations of lighting between sample images in DIA, however a wider comparison between image-processing methods in DIA for chemical quantification is warranted.

4.2 Comparison with other DIA methods for investigation of DOC concentration

Digital image analysis for estimation of DOC concentration has been reported previously for coastal and freshwaters. Goddijn *et al.*, (2006) and Goddijn-Murphy *et al.*, (2009)[36,65] demonstrated a relationship between R/G values from *in situ* digital images with the absorption coefficient at 440 nm of Irish coastal waters. The authors used a custom apparatus for underwater measurements, with associated uncertainty of ~20%. Zeng *et al.*, (2021)[38] developed a methodology using smartphone imaging with a low cost, custom-built sample enclosure. This device demonstrated a strong negative relationship between RGB pixel intensity and a derived chromaticity index with increasing humic acid concentration in artificial freshwater samples, but the authors did not estimate the concentration of DOC or humic acid in environmental samples. The HydroColour app[35] uses RGB image data to estimate the above water remote sensing reflectance (R_{rs}) of coastal waters, which is influenced by water turbidity and the concentrations of DOC and chlorophyll. The R_{rs} estimated from smartphone RGB image data showed a strong correlation to the results of a reference instrumental method, with associated error of 16–26%. These examples identify the potential for DIA in the estimation of water chemical properties, and also highlight the gap in the published literature for a simple smartphone based method for the analysis of DOC in freshwaters. The accuracy of the Cup of Carbon method using replicate sample measurements for estimation of DOC in freshwaters was within 8.2 ± 26.2% (−0.24 ± 2.07 mg L^{-1}) of the true DOC concentration (Fig. 7), which is in good agreement with the published examples described above. Digital image analysis methods tend to have poorer precision than standard laboratory methods even with a variety of hardware adjustments and image processing techniques applied.[23,63] For example, replicate DOC measurements using a TOC analyzer typically have RSD of <2%, while the UV/Vis absorbance

methods typically have RSD <5%, which are much lower than the RSD for B_{ws} shown in Table 1 of up to 30%. However, despite having poorer accuracy and precision than standard laboratory methods, DIA methods can show acceptable accuracy if replicate measurements are used,[34] as seen in Fig. 7. In addition, with 10 replicate measurements, the precision of the Cup of Carbon method was good enough to identify significant differences between samples with moderate differences in DOC concentration of ~4 mg L^{-1} (section 3.2.1 and SI 4). The accuracy and precision of the Cup of Carbon method makes it appropriate for the estimation of DOC concentration in citizen science and other resource-limited settings, however it is not intended as a replacement for standard laboratory methods for robust quantification of environmental samples.

4.3 Potential interferences with DOC estimation by the Cup of Carbon method

The Cup of Carbon method proved to be effective for the estimation of DOC in clear waters around the Silver Flowe peatland, however other water quality parameters, such as turbidity, Fe(III) concentration, and chlorophyll-a concentration, also impact the optical properties of water samples.[35,66,67] If samples are turbid, a simple filtration step using qualitative filter papers would be likely to remove any interfering suspended solid particles and make the Cup of Carbon analysis possible. However, this was not tested in the current study as filtration was not required due to the negligible concentrations of suspended particles encountered (SI 3). The contribution of chlorophyll-a to water colour or absorbance is generally low and requires a significant concentration step to be measurable.[68] In particular, the amount of photosynthetic algae is unlikely to be high in the upland streams around peatlands due to low nutrient concentrations, low pH, and limited light penetration into dark waters.[69] However, under eutrophic conditions high concentrations of photosynthetic algae could potentially impact the DOC estimation by the Cup of Carbon method. Fe(III) shows similar absorbance characteristics to DOC and therefore can lead to the over-estimation of DOC from absorbance or colour-based methods.[40,66] Eleven of the water samples measured in this study also had TOC quantified by a standard method (TOC analyzer, Thermolox, Sercon) which showed excellent agreement with the UV/Vis estimate of DOC concentration (see SI 2), suggesting that this was not a problematic issue in the results presented. It is possible that DOC concentration could also be over-estimated by the Cup of Carbon method in samples with high Fe(III) concentration, however Fe(III) tends to make a lesser contribution to the brown colour of water compared to DOC.[40] The potential influence of Fe(III) on the estimates of DOC using the Cup of Carbon method and the method ability to estimate DOC in turbid samples after filtration are worthy of further investigation to expand the applicability of the method to water samples from other areas.

4.4 Application in citizen science and further routes for optimization

Methods using DIA often consider citizen science as a useful potential application,[23,28,34,35,38,63] however there are relatively few published studies reporting the use of DIA methods for chemical analysis under field conditions by different users with different smartphones. Leeuw and Boss (2018)[35] report one of few published examples which presents the results from the application of smartphone-based DIA in citizen science to estimate the turbidity of coastal waters. Often, smartphone based DIA methods for water analysis require additional hardware adaptations for smartphones which may use bespoke or 3D printed components, or require chemicals to react with an analyte of interest which may be barriers to their uptake in citizen science. Methods using sample enclosures made from readily available recycled materials help to make methods more accessible while improving the reproducibility of results,[23,70,71] however the requirement to construct an enclosure before analysis may still discourage potential users from applying the methods. Like the method of Leeuw and Boss (2018),[35] a key benefit of the Cup of Carbon method is the fact that it requires minimal equipment using only a ceramic mug with white interior, a laminated piece of white paper, and a digital camera, such as a smartphone camera. This makes the method uniquely suited for citizen science, education and other resource-limited settings where costly equipment or bespoke sample enclosures may be a barrier to potential users. In addition, the Cup of Carbon Shiny app (available with the SI), incorporating the novel B_{ws} image processing and calibration, allows quick and easy image processing and analysis, enabling rapid conversion of digital images to estimated DOC concentration. The comparison of the results from different phones using LMMs indicated that the results from different phones are comparable. However, best results are likely to be achieved by use of a single analyst using one phone and one mug, ensuring equal height from each sample and taking several repeat photographs of each sample. This protocal minimises the variation and error added with multiple users with different equipment and technique. In addition, the creation of a calibration card with coloured squares covering the working range of water DOC colour from 0–35 mg L^{-1} could be used to create an in-field calibration to take local lighting conditions into account during sample analysis.[49] The accessibility of the method could be further improved by the development of a smartphone app to handle all the required image capture, processing and data analysis steps.[34,64,72] This would also enable better control of camera functionality, such as ensuring the flash is turned off, ensuring that no digital filters are applied to images, and maximising image resolution, which is known to improve DIA methods compared to the use of compressed image formats.[73] It may be possible to expand the working range of the method by exploring the G pixel intensity at higher concentrations, or by applying a dilution step to very dark water samples with colourless water, such as tap water, bottled water or deionised water.

Finally, the potential interferences from Fe(III) and turbidity, and additional ways to improve the reproducibility of the method would benefit from further detailed investigation. The Cup of Carbon method represents a promising approach for the estimation of DOC concentration in coloured waters for citizen science, education, and outreach settings, and further development could lead to improvements in accuracy and precision to broaden the applications of the method.

5 Conclusion

The novel Cup of Carbon method uses a simple and user-friendly digital image analysis method for estimation of the concentration of dissolved organic carbon in coloured freshwaters from peatlands. RGB analysis of images of peatland water samples in a ceramic mug with a white interior showed a negative logarithmic relationship between B pixel intensity and DOC concentration. The novel white subtraction image processing method improved accuracy and enabled good estimates to be made of DOC concentration in a range of ~1–35 mg L^{-1}. Calculating the average of replicate measurements enabled DOC to be estimated with good accuracy and acceptable precision using 8 different smartphones on two visits to the Silver Flowe peatland in Galloway. The Cup of Carbon method is ideally suited for monitoring of DOC concentrations in peatland surface waters as part of citizen science or educational outreach activities due to the basic equipment requirement of a smartphone with digital camera, ceramic mug with white interior and laminated sheet of white paper. The open source Cup of Carbon Shiny computer app allows fast analysis of images to estimate DOC concentration. The Cup of Carbon method is one of only a small number of published examples of DIA methods being used in the field for investigating water quality as part of a citizen science activity, and this study highlights the potential for smartphone-based DIA methods to expand the availability of analytical methods to a broad range of users.

Author contributions

M. M.: conceptualization, methodology, formal analysis, investigation, writing – original draft, visualization. L. R., K. M., K. G., and E. T.: investigation, project administration, funding acquisition. A. B.: investigation, resources.

Conflicts of interest

The authors have no conflicts of interest to declare.

Data availability

Data for this article including R code for the Cup of Carbon Shiny app, example Cup of Carbon images, the calibration and analytical data used in this study, and details of the quality control for the dissolved organic carbon measurement are available from Github: https://github.com/MMuirEnvSci/CupOfCarbon and archived on Zenodo: https://doi.org/10.5281/zenodo.15861929.

Supplementary information (SI) is available. See DOI: https://doi.org/10.1039/d5an00738k.

Acknowledgements

Part of the "Peatland Connections" project: https://www.peatlandconnections.com, funded by the Galloway Glens Landscape Partnership, the Esmée Fairbairn Foundation and the National Lottery Heritage Fund. Thanks to Forestry and Land Scotland for allowing access to the site.

References

1 N. D. Ward, T. S. Bianchi, P. M. Medeiros, M. Seidel, J. E. Richey, R. G. Keil and H. O. Sawakuchi, *Front. Mar. Sci.*, 2017, **4**, 7, DOI: 10.3389/fmars.2017.00007.
2 A. Nebbioso and A. Piccolo, *Anal. Bioanal. Chem.*, 2013, **405**, 109–124, DOI: 10.1007/s00216-012-6363-2.
3 C. S. Hopkinson Jr and J. J. Vallino, *Nature*, 2005, **433**, 142–145, DOI: 10.1038/nature03191.
4 F. L. Brailsford, H. C. Glanville, P. N. Golyshin, P. J. Johnes, C. A. Yates and D. L. Jones, *Sci. Rep.*, 2019, **9**, 11229, DOI: 10.1038/s41598-019-47749-6.
5 M. Erlandsson, N. Cory, S. Köhler and K. Bishop, *J. Geophys. Res.: Biogeosci.*, 2010, **115**, 1–8, DOI: 10.1029/2009JG001082.
6 J. Beaulne, M. Garneau, G. Magnan and É. Boucher, *Sci. Rep.*, 2011, **11**, 2657, DOI: 10.1038/s41598-021-82004-x.
7 M. G. Evans, D. M. Alderson, C. D. Evans, A. Stimson, T. E. Allott, C. Goulsbra, F. Worrall, T. Crouch, J. Walker, M. H. Garnett and J. Rowson, *J. Geophys. Res.: Biogeosci.*, 2022, **127**, 1–19, DOI: 10.1029/2021JG006344.
8 T. Cummins and E. P. Farrell, *For. Ecol. Manage*, 2003, **180**, 557–570, DOI: 10.1016/S0378-1127(02)00649-7.
9 J. L. Williamson, A. Tye, D. J. Lapworth, D. Monteith, R. Sanders, D. J. Mayor, C. Barry, M. Bowes, M. Bowes, A. Burden, N. Callaghan, G. Farr, S. Felgate, A. Fitch, S. Gibb, P. Gilbert, G. Hargreaves, P. Keenan, V. Kitidis, M. Juergens, A. Martin, I. Mounteney, P. D. Nightingale, M. G. Pereira, J. Olszewska, A. Pickard, A. P. Rees, B. Spears, M. Stinchcombe, D. White, P. Williams, F. Worrall and C. Evans, *Biogeochemistry*, 2021, **164**, 163–184, DOI: 10.1007/s10533-021-00762-2.
10 A. M. Bass, M. Coleman, S. Waldron and M. Scott, *Limnol. Oceanogr.*, 2023, **68**, 1750–1761, DOI: 10.1002/lno.12382.
11 K. Heal, A. Phin, S. Waldron, H. Flowers, P. Bruneau, A. Coupar and A. Cundill, *Ambio*, 2020, **49**, 442–459, DOI: 10.1007/s13280-019-01200-2.

12 J. Xu, P. J. Morris, J. Liu, J. L. Ledesma and J. Holden, *Water Resour. Res.*, 2020, **56**, 1–19, DOI: 10.1029/2019WR025592.
13 S. J. Ramchunder, L. E. Brown and J. Holden, *J. Appl. Ecol.*, 2012, **49**, 182–191, DOI: 10.1111/j.1365-2664.2011.02075.x.
14 D. T. Monteith, A. G. Hildrew, R. J. Flower, P. J. Raven, W. R. Beaumont, P. Collen, A. M. Kreiser, E. M. Shilland and J. H. Winterbottom, *Environ. Pollut.*, 2005, **137**, 83–101, DOI: 10.1016/j.envpol.2004.12.026.
15 I. Serrano, I. Buffam, D. Palm, E. Brännäs and H. Laudon, *Trans. Am. Fish. Soc.*, 2008, **137**, 1363–1377, DOI: 10.1577/T07-069.1.
16 H. Laudon and I. Buffam, *Hydrol. Earth Syst. Sci.*, 2008, **12**, 425–435, DOI: 10.5194/hess-12-425-2008.
17 R. van der Wal, A. Bonn, D. Monteith, M. Reed, K. Blackstock, N. Hanley, D. Thompson, M. Evans, I. Alonso, T. Allott, H. Armitage, N. Beharry, J. Glass, S. Johnson, J. Mcmorrow, L. Ross, R. Pakeman, S. Perry and D. Tinch, The UK National Ecosystem Assessment Technical Report, UNEP-WCMN, 2011, pp. 105–159.
18 J. Williamson, C. Evans, B. Spears, A. Pickard, P. J. Chapman, F. Leith, S. Waldron and D. Monteith, *Biogeosciences*, 2022, **209**, 1–24, DOI: 10.5194/bg-2022-209.
19 J. P. Ritson, N. J. Graham, M. R. Templeton, J. M. Clark, R. Gough and C. Freeman, *Sci. Total Environ.*, 2014, **473–474**, 714–730, DOI: 10.1016/j.scitotenv.2013.12.095.
20 A. T. S. Chow, Y. Ulus, G. Huang, M. A. Kline and W. Y. Cheah, *J. Environ. Qual.*, 2022, **51**, 837–871, DOI: 10.1002/jeq2.20392.
21 M. Peacock, C. D. Evans, N. Fenner, C. Freeman, R. Gough, T. G. Jones and I. Lebron, *Environ. Sci.: Processes Impacts*, 2014, 10–12, DOI: 10.1039/c4em00108g.
22 H. T. Carter, E. Tipping, J. F. Koprivnjak, M. P. Miller, B. Cookson and J. Hamilton-Taylor, *Water Res.*, 2012, **46**, 4532–4542, DOI: 10.1016/j.watres.2012.05.021.
23 M. R. Muir and A. Innes, *Anal. Methods*, 2024, **16**, 5571–5583, DOI: 10.1039/d4ay00991f.
24 Y. Fan, J. Li, Y. Guo, L. Xie and G. Zhang, *Measurement*, 2021, **171**, 108829, DOI: 10.1016/j.measurement.2020.108829.
25 K. E. McCracken and J. Y. Yoon, *Anal. Methods*, 2016, **8**, 6591–6601, DOI: 10.1039/c6ay01575a.
26 D. V. Baker, J. Bernal-Escalante, C. Traaseth, Y. Wang, M. V. Tran, S. Keenan and W. R. Algar, *Lab Chip*, 2025, **25**, 884–955, DOI: 10.1039/d4lc00966e.
27 K. Golicz, S. Hallett, R. Sakrabani and J. Ghosh, *Comput. Electron. Agric.*, 2020, **175**, 105532, DOI: 10.1016/j.compag.2020.105532.
28 S. Zheng, H. Li, T. Fang, G. Bo, D. Yuan and J. Ma, *Sci. Total Environ.*, 2022, **815**, 152613, DOI: 10.1016/j.scitotenv.2021.152613.
29 M. L. Firdaus, W. Alwi, F. Trinoveldi, I. Rahayu, L. Rahmidar and K. Warsito, *Proc. Environ. Sci.*, 2014, **20**, 298–304, DOI: 10.1016/j.proenv.2014.03.037.
30 L. Shen, J. A. Hagen and I. Papautsky, *Lab Chip*, 2012, **12**, 4240–4243, DOI: 10.1039/c2lc40741h.
31 S. Odenwald, *Citizen Science: Theory and Practice*, 2019, **4**, 18, DOI: 10.5334/cstp.158.
32 D. Fraisl, G. Hager, B. Bedessem, M. Gold, P. Y. Hsing, F. Danielsen, C. B. Hitchcock, J. M. Hulbert, J. Piera, H. Spiers, M. Thiel and M. Haklay, *Nat. Rev. Methods Primers*, 2022, **2**, 1–20, DOI: 10.1038/s43586-022-00144-4.
33 N. A. Welden, P. A. Wolseley and M. R. Ashmore, *Environ. Pollut.*, 2018, **232**, 80–89, DOI: 10.1016/j.envpol.2017.09.020.
34 T. J. Malthus, R. Ohmsen and H. J. van der Woerd, *Remote Sens.*, 2020, **12**, 1–20, DOI: 10.3390/rs12101578.
35 T. Leeuw and E. Boss, *Sensors*, 2018, **18**(256), 1–15, DOI: 10.3390/s18010256.
36 L. M. Goddijn and M. White, *Estuarine, Coastal Shelf Sci.*, 2006, **66**, 429–436, DOI: 10.1016/j.ecss.2005.10.002.
37 R. Schima, S. Krüger, J. Bumberger, M. Paschen, P. Dietrich and T. Goblirsch, *Front. Earth Sci.*, 2019, **7**, 184, DOI: 10.3389/feart.2019.00184.
38 R. Zeng, C. M. Mannaerts and Z. Shang, *Sensors*, 2021, **21**, 6699, DOI: 10.3390/s21206699.
39 L. E. Parry, P. J. Chapman, S. M. Palmer, Z. E. Wallage, H. Wynne and J. Holden, *Sci. Total Environ.*, 2015, **527–528**, 530–539, DOI: 10.1016/j.scitotenv.2015.03.036.
40 G. A. Weyhenmeyer, Y. T. Prairie and L. J. Tranvik, *PLoS One*, 2014, **9**, e88104, DOI: 10.1371/journal.pone.0088104.
41 Crichton Carbon Centre, *Peatland Connections*, 2023, https://www.peatlandconnections.com.
42 Ramsar, *Silver Flowe*, 2005, https://rsis.ramsar.org/ris/219.
43 *R: A Language and Environment for Statistical Computing*, 2023, https://www.R-project.org/.
44 *Posit, RStudio: Integrated Development Environment for R, Posit Software*, PBC, Boston, MA, 2023.
45 W. Chang, J. Cheng, J. Allaire, C. Sievert, B. Schloerke, Y. Xie, J. Allen, J. McPherson, A. Dipert and B. Borges, *shiny: Web Application Framework for R*, 2025.
46 T. L. Pedersen, *shinyFiles: A Server-Side File System Viewer for Shiny*, 2022.
47 S. Barthelme, D. Tschumperle, J. Wijffels, H. E. Assemlal, S. Ochi, A. Robotham and R. Tobar, *imager: Image Processing Library Based on 'CImg'*, 2024.
48 J. A. S. Viggiano, *Proc. SPIE 5301, Sensors and Camera Systems for Scientific, Industrial, and Digital Photography Applications V*, 2004.
49 L. de Greef, M. Goel, M. J. Seo, E. C. Larson, J. W. Stout, J. A. Taylor and S. N. Patel, UbiComp '14, Proceedings of the 2014 ACM International Joint Conference on Pervasive and Ubiquitous Computing, 2014, pp. 331–342, DOI: 10.1145/2632048.2632076.
50 *Microsoft Excel*, https://office.microsoft.com/excel, 2024.
51 *Minitab LLC*, https://www.minitab.com, 2023.
52 D. G. Altman, *Practical Statistics for Medical Research*, Chapman & Hall/CRC, 1st edn, 1991, ch. 9, pp. 179–223.
53 L. Lin, *Biometrics*, 1989, **45**, 255–268, DOI: 10.2307/2532051.
54 L. Lin, A. S. Hedayat and W. Wu, *Statistical Tools for Measuring Agreement*, Springer, 2012, ch. 2, pp. 7–54.

55 A. Signorelli, *DescTools: Tools for Descriptive Statistics*, 2017.
56 D. W. Meek, T. A. Howell and C. J. Phene, *Agron. J.*, 2009, **101**, 1012–1018, DOI: 10.2134/agronj2008.0180x.
57 D. Bates, M. Mächler, B. M. Bolker and S. C. Walker, *J. Stat. Softw.*, 2015, **67**(1), 1–48, DOI: 10.18637/jss.v067.i01.
58 A. Kuznetsova, P. B. Brockhoff and R. H. B. Christensen, *J. Stat. Softw.*, 2017, **82**(13), 1–26, DOI: 10.18637/jss.v082.i13.
59 D. Kong, J. Zhao, S. Tang, W. Shen and H. K. Lee, *Anal. Chem.*, 2021, **93**, 12156–12161, DOI: 10.1021/acs.analchem.1c02011.
60 M. N. Azhar, A. Bustam, F. S. Naseem, S. S. Shuin, M. H. Md Yusuf, N. U. Hishamudin and K. Poh, *Digital Health*, 2023, **9**, 1–11, DOI: 10.1177/20552076231154684.
61 M. Nixon, F. Outlaw and T. S. Leung, *PLoS One*, 2020, **15**, e0230561, DOI: 10.1371/journal.pone.0230561.
62 L. P. dos Santos Benedetti, V. B. dos Santos, T. A. Silva, E. B. Filho, V. L. Martins and O. Fatibello-Filho, *Anal. Methods*, 2015, **7**, 4138–4144, DOI: 10.1039/c5ay00529a.
63 K. Golicz, S. H. Hallett, R. Sakrabani and G. Pan, *Sci. Rep.*, 2019, **9**, 1–10, DOI: 10.1038/s41598-019-52702-8.
64 M. Aitkenhead, D. Donnelly, M. Coull and R. Gwatkin, *Digital Soil Morphometrics*, Springer, 2016, ch. 7, pp. 89–110, DOI: 10.1007/978-3-319-28295-4_7.
65 L. Goddijn-Murphy, D. Dailloux, M. White and D. Bowers, *Sensors*, 2009, **9**, 5825–5843, DOI: 10.3390/s90705825.
66 L. A. Logozzo, J. W. Martin, J. McArthur and P. A. Raymond, *Biogeochemistry*, 2022, **160**, 17–33, DOI: 10.1007/s10533-022-00937-5.
67 W. Ren, X. Wu, J. Chao, X. Ge, S. Zhu and M. Zhou, *J. Freshwater Ecol.*, 2022, **37**, 243–257, DOI: 10.1080/02705060.2022.2045231.
68 Chlorophyll-A, in *Standard Methods For the Examination of Water and Wastewater*, ed. W. Lipps, T. Baxter and E. Braun-Howland, Standard Methods Committee of the American Public Health Association, American Water Works Association, Water Environment Federation, 2018, ch. 10150.
69 R. M. Pilla and N. A. Griffiths, *Ecosystems*, 2024, **27**, 137–150, DOI: 10.1007/s10021-023-00878-6.
70 M. de O. K. Franco, W. J. Cardoso, C. B. Vilanculo, V. B. dos Santos, J. P. B. de Almeida, L. F. Capitán-Vallvey and W. T. Suarez, *Anal. Methods*, 2023, **15**, 2287–2400, DOI: 10.1039/d3ay00311f.
71 B. S. Hosker, *J. Chem. Educ.*, 2018, **95**, 178–181, DOI: 10.1021/acs.jchemed.7b00548.
72 R. Lemmens, V. Antoniou, P. Hummer, C. Potsiou, R. Lemmens, V. Antoniou, P. Hummer and C. Potsiou, *The Science of Citizen Science*, 2021, ch. 23, pp. 461–474, DOI: 10.1007/978-3-030-58278-4_23.
73 O. Burggraaff, M. Werther, E. S. Boss, S. G. Simis and F. Snik, *Front. Remote Sens.*, 2022, **3**, 940096, DOI: 10.3389/frsen.2022.940096.